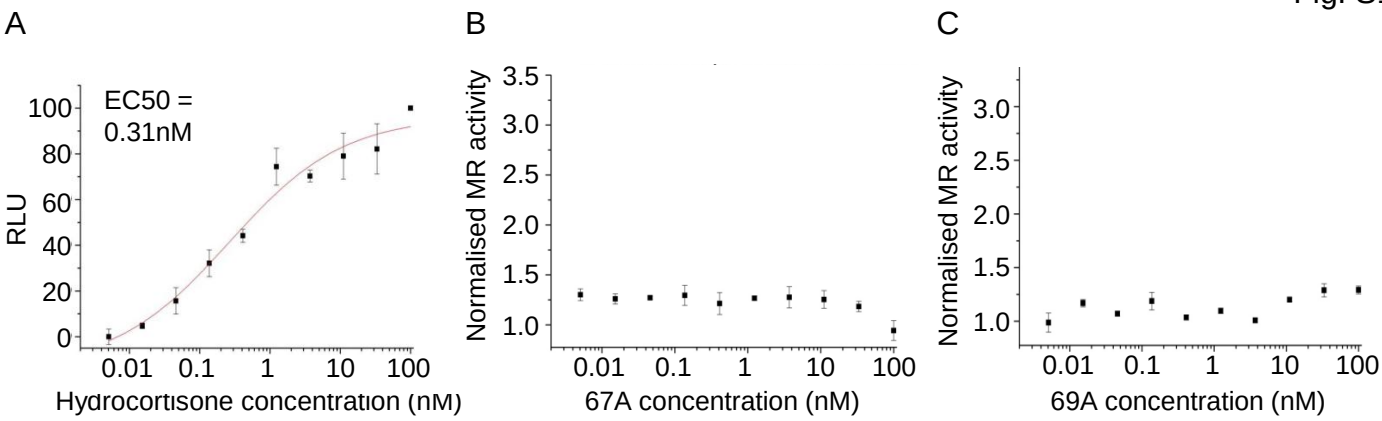

Fig. S1: NSGs are highly GR specific

MR transactivation assays for GSK47867A [67A] and GSK47869A [69A] (B and C) relative to a hydrocortisone control (A). The EC50 value for hydrocortisone is given in the upper left. RLU are normalised between 0 (no activity) and 100 (full activity) and the EC50 values were determined by GraphPad Prism software, n=3.

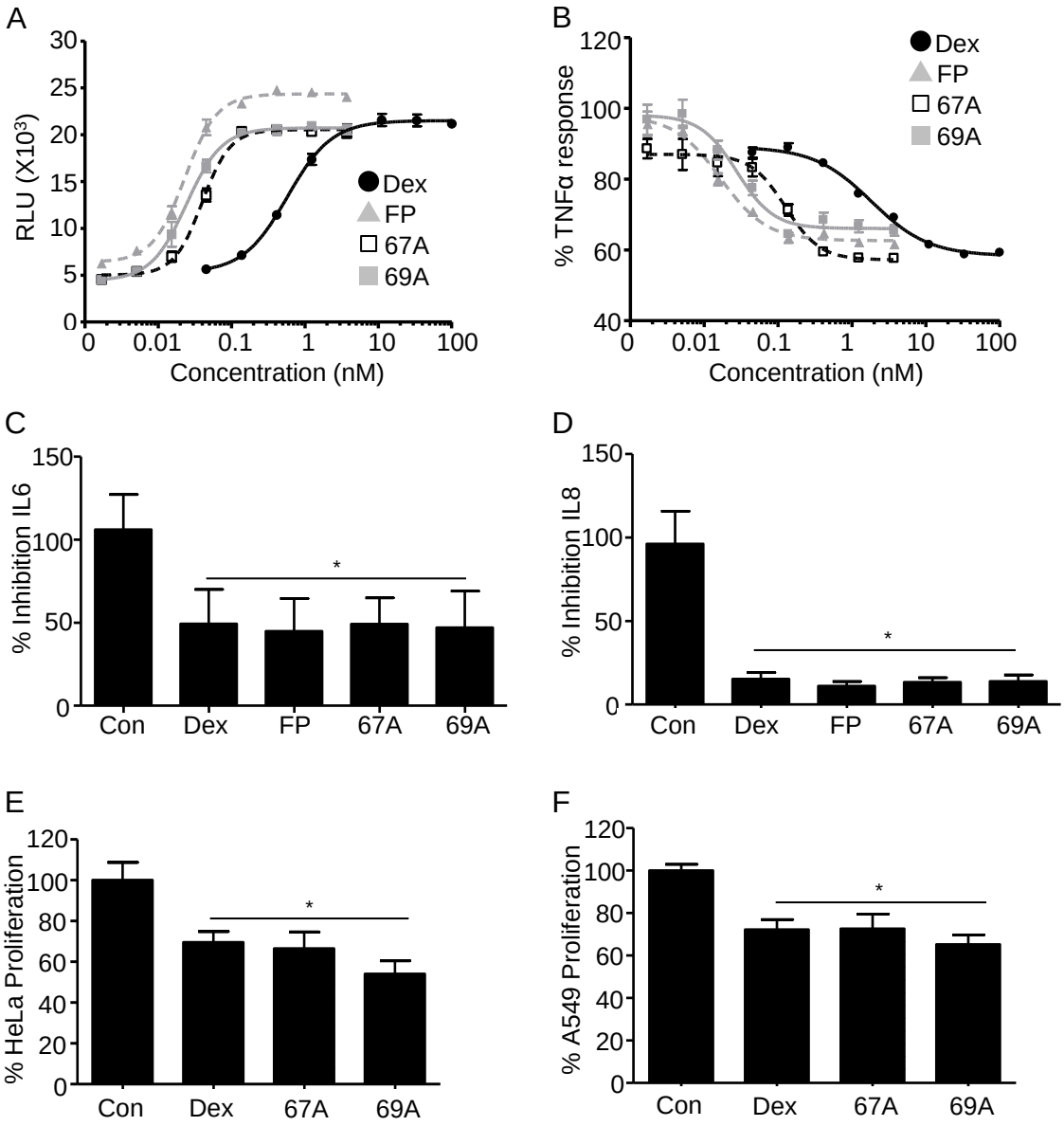

Fig.S2: The NSGs are highly potent

A549 cells stably expressing a GRE-Luc (A) or NFκB-Luc (B) were used to confirm the results found in HeLa (Figure 1 B,C). A549 cells were treated with 0.01-1000 nM Dex, FP, GSK47867A [67A] or GSK47869A [69A] for eighteen hours then lysed and subjected to analysis by luciferase assay. Graph (mean ± SD) shows the relative light units (RLU) (A) or % TNFα response (B) from one of three representative experiments performed in triplicate. A549 cells were incubated with DMSO, 100 nM Dex, 3 nM FP, 3 nM 67A or 3 nM 69A for eighteen hours. Following treatment supernatants were collected and assayed for IL6 (C) and IL8 (D) concentration using a Luminex 100 with StarStation software. Graphs (mean ± SEM) show % inhibition of IL6 and IL8 production. HeLa and A549 cells were treated with DMSO vehicle, 100 nM Dex, 3 nM 67A or 3 nM 69A for seventy two hours. Subsequently MTS reagent was added to the treated cells and the formazan production was measured after two hours at a wavelength of 490nm. Graphs show formazan production for each treatment which directly correlates to the number of viable cells (E,F). Statistical significance was evaluated by one way ANOVA followed by Tukey post-test. Asterisks indicate: *p < 0.001 significantly different from vehicle treated control.

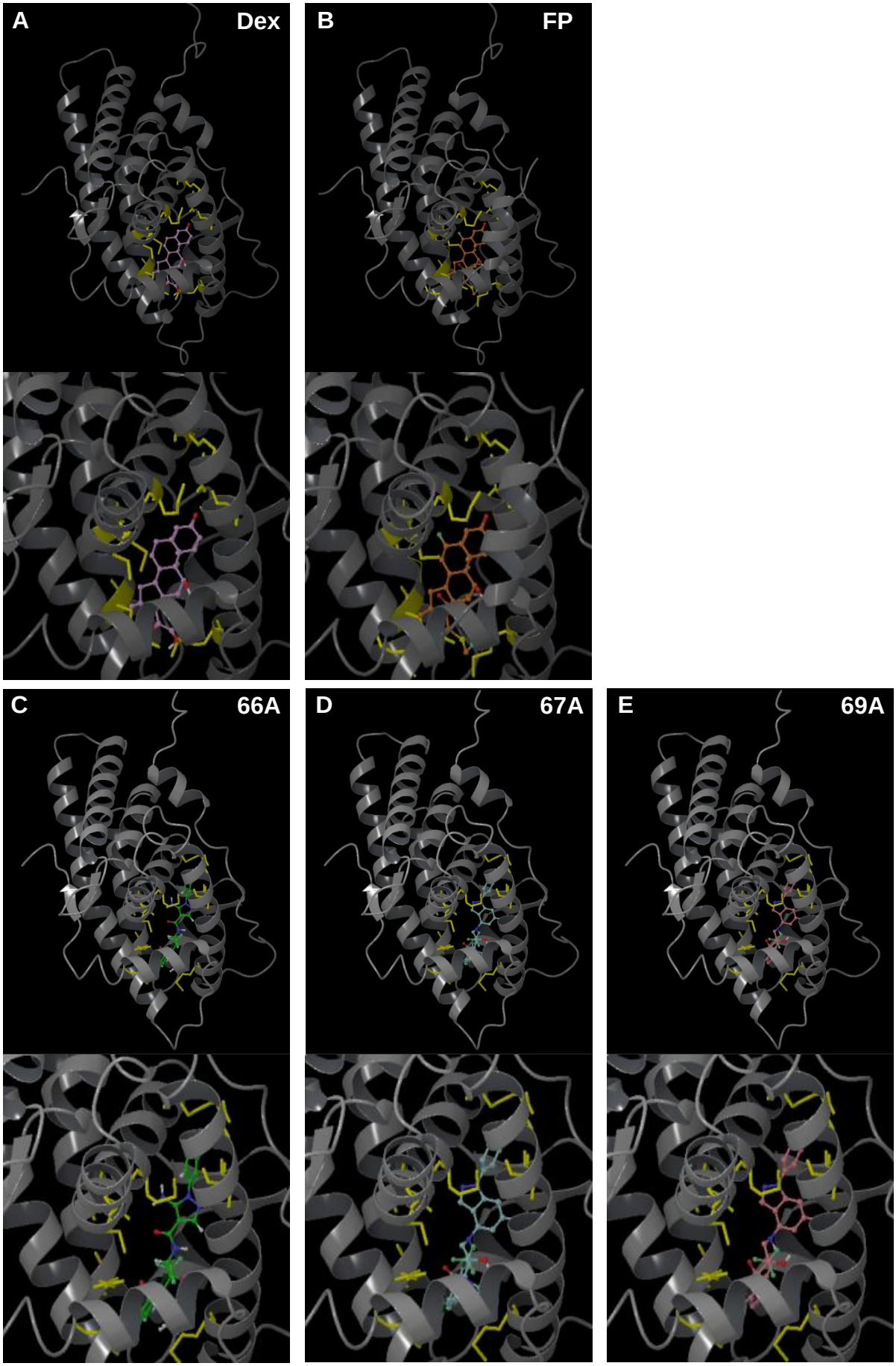

Fig.S3: Docking NSG into GR LBD crystal structure

Comparison of the crystal structures of the GR LBD bound to Dex (A, purple), FP (B, orange) and GSK47866A [66A] (C, green). GSK47867A [67A] (D, blue) and GSK47869A [69A] (E, Pink) were docked into the binding pocket of 66A and gave a very high scoring fit. The residues in the binding pocket that show significant movement with NSG binding are highlighted in yellow.

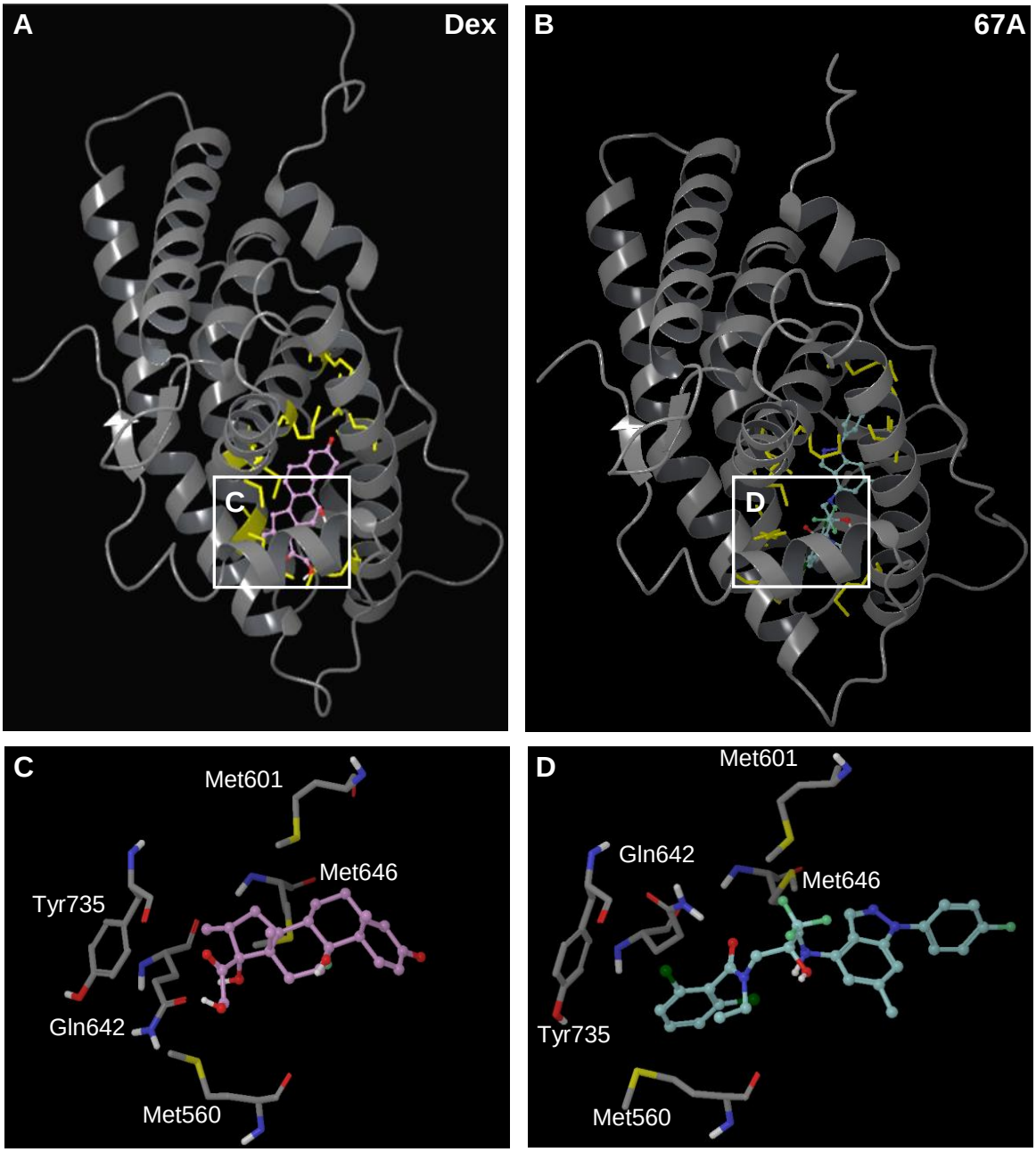

Fig.S4: Movement of residues at tail of ligand (D ring).
Comparison of the crystal structures of the GR LBD bound to Dex (A, purple) and GSK47867A [67A] (B, Blue). The residues in the binding pocket that show significant movement upon 67A binding are highlighted in yellow. When 67A binds to the GR LBD the tail region of the ligand causes movement of residues Met560, Met601, Gln642, Met 646 and Tyr 735 (D) when compared with Dex (C).

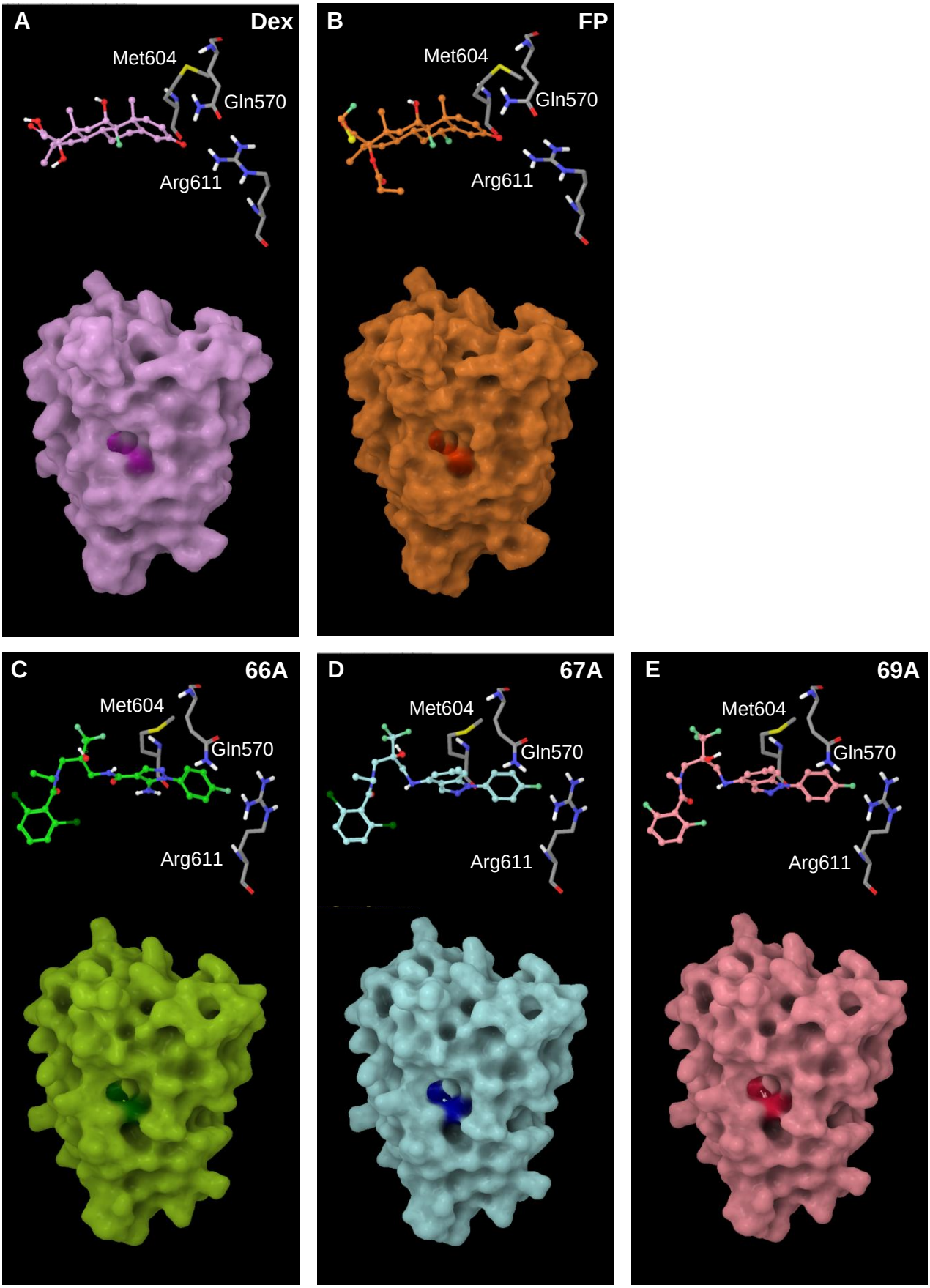

Fig.S5: Comparison of GR LBD surface with steroidal and non-steroidal ligands at the head end of the ligand (A ring)

Comparison of the crystal structures of the GR LBD bound to Dex (A, purple), FP (B, orange), GSK47866A [66A] (C, green), GSK47867A [67A] (D, blue) and GSK47869A [69A] (E, pink). The region of the GR LBD surface where residues Gln570, Met604 and Arg611 are exposed is highlighted.

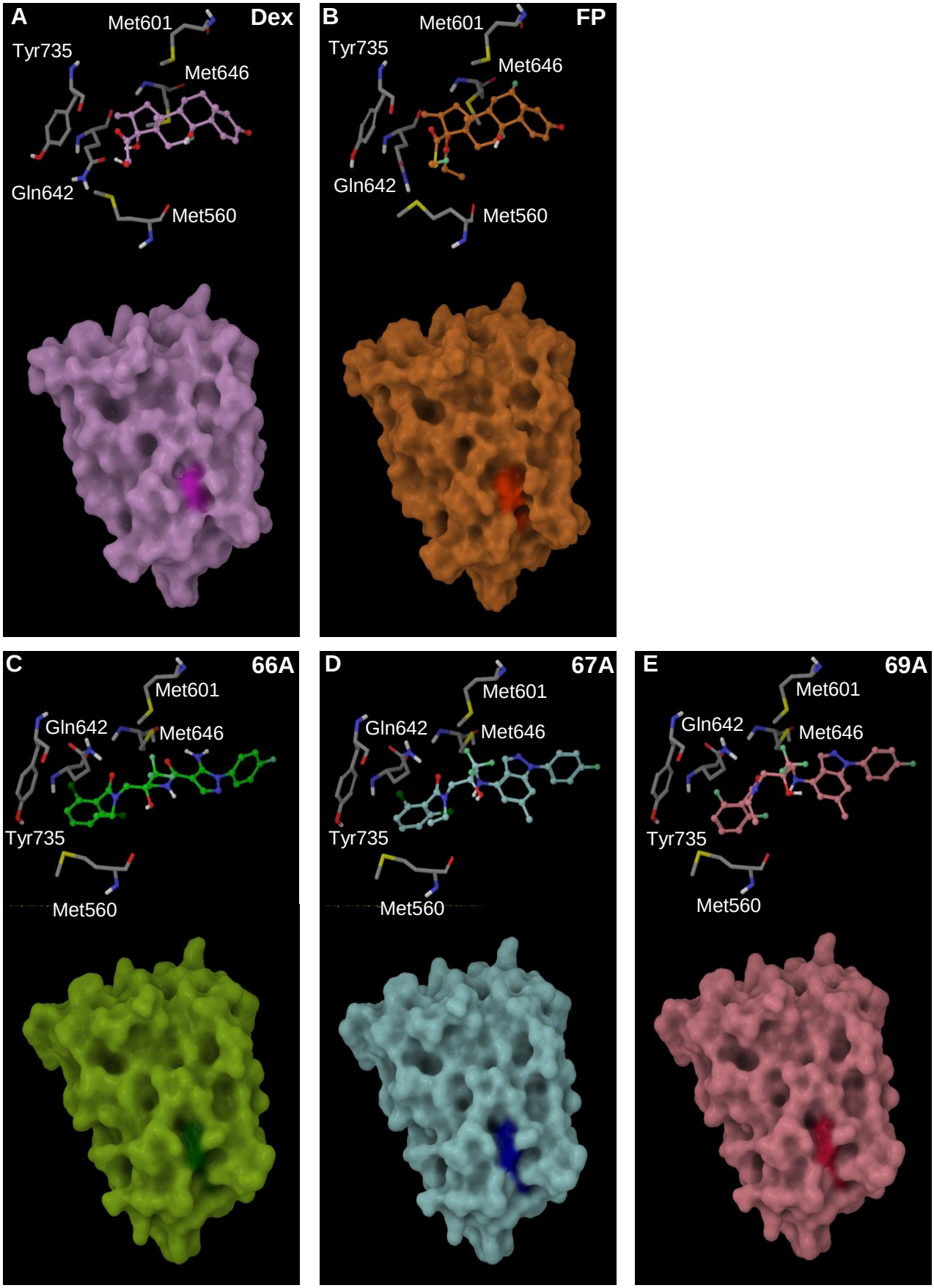

Fig.S6: Comparison of GR LBD surface with steroidal and non-steroidal ligands at the tail end of the ligand (D ring)

Comparison of the crystal structures of the GR LBD bound to Dex (A, purple), FP (B, orange), GSK47866A [66A] (C, green), GSK47867A [67A] (D, blue) and GSK47869A [69A] (E, pink). When the NSGs bind to the GR LBD the tail region of the ligands cause movement of residues Met560, Met601, Gln642, Met 646 and Tyr 735. The region of the GR LBD surface where residues Met560, Gln642 and Tyr735 and are exposed is highlighted.

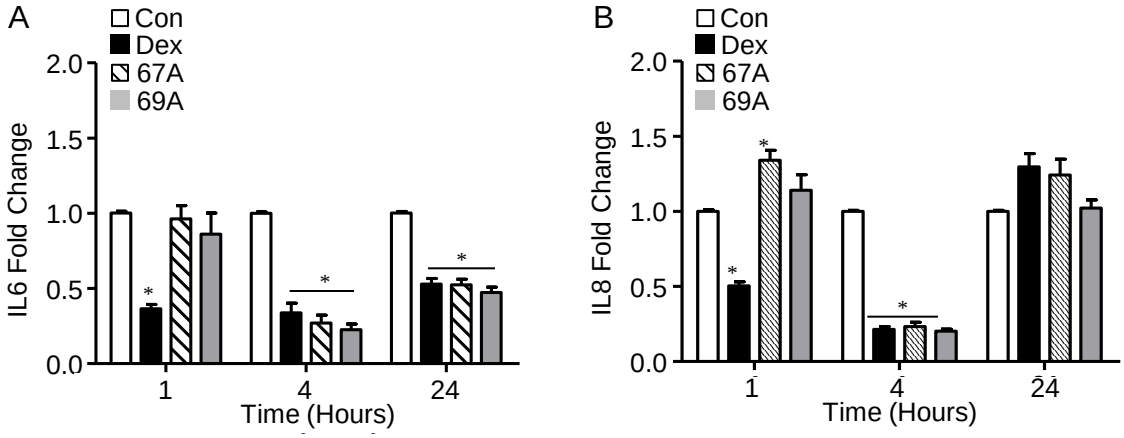

Fig.S7: Regulation of endogenous genes IL6 and IL8.
HeLa cells were treated with TNF α 5 ng/ml, DMSO vehicle, 100 nM Dex, 3 nM GSK47867A [67A] or 3 nM GSK47869A [69A] for one, four or twenty four hours then lysed and RNA extracted using an RNeasy kit. RNA was reverse transcribed and subjected to qPCR IL6 (A) or IL8 (B) using Sybr Green detection in an ABI q-PCR machine and data analysed by δδ CT method. Graphs (mean ± SEM) combine data from three separate experiments and display fold change over vehicle treated control. Statistical significance was evaluated by one way ANOVA followed by Tukey post-test. Asterisks indicate: *$p < 0.005$ significantly different from control.

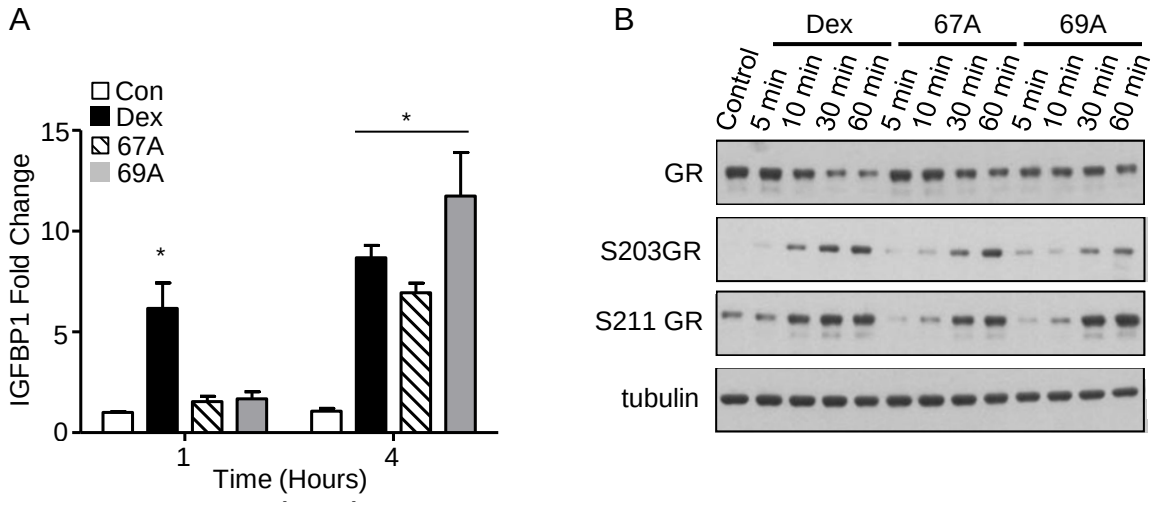

Fig.S8: Kinetics of GR phosphorylation

HeLa cells were treated with DMSO vehicle, 100 nM Dex, 3 nM GSK47867A [67A] or 3 nM GSK47869A [69A] for one or four hours then lysed and RNA extracted using an RNeasy kit. RNA was reverse transcribed and subjected to qPCR of IGFBP1 (A) using Sybr Green detection in an ABI q-PCR machine and data analysed by δδ CT method. Graph (mean ± SEM) combines data from two separate experiments and displays fold change over vehicle treated control. HeLa cells were treated either with 100 nM Dex or 3 nM 67A or 69A for up to sixty minutes then lysed in RIPA buffer containing phosphatase and protease inhibitors and analysed by immunoblotting for GR abundance, GR ser 203 and GR ser 211 phosphorylation (B). α-Tubulin was used as a loading control. Statistical significance was evaluated by one way ANOVA followed by Tukey post-test. Asterisks indicate: *$p < 0.005$ significantly different from control.

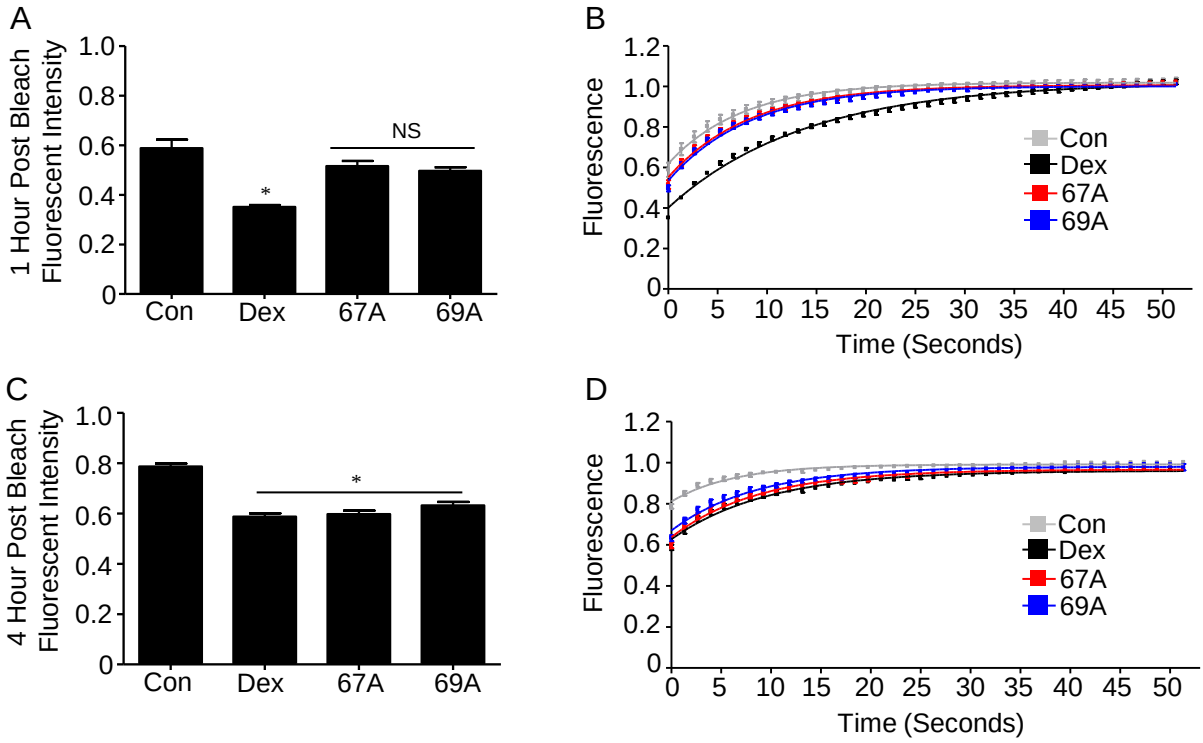

Fig.S9. GR nuclear mobility

HeLa cells were transfected with GR-GFP and incubated with 100 nM Dex, 3 nM GSK47867A [67A] or 3 nM GSK47869A [69A] for one (A,B) or four hours (C,D). The nuclei of the treated cells were subjected to photobleaching and the level of bleach (A, C) and time to recovery (B, D) was measured for each treatment. Statistical significance was evaluated by one way ANOVA followed by Tukey post-test. Asterisks indicate: *$p < 0.001$ significantly different from control.

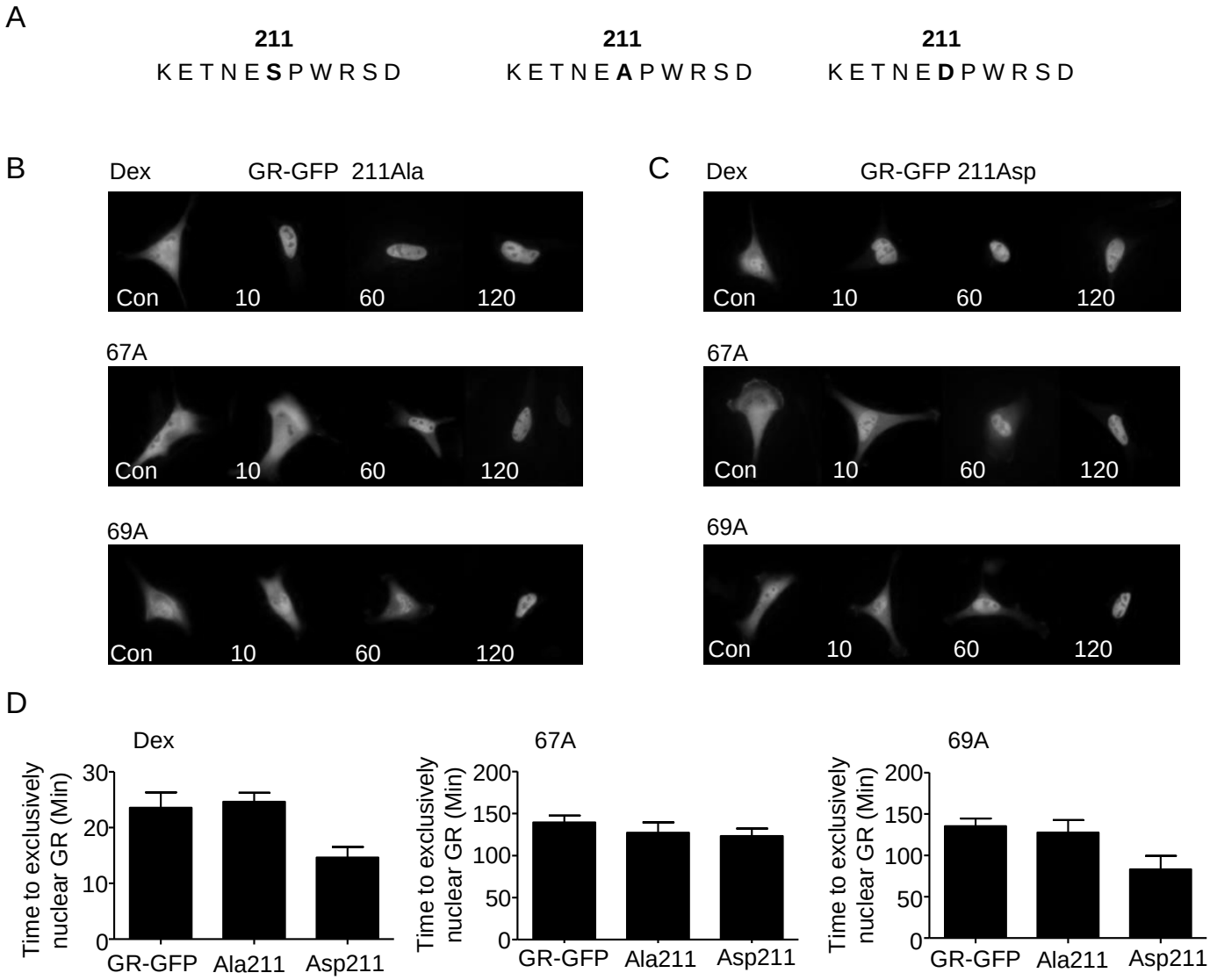

Fig.S10: GR translocation with 211 phospho mutants

Schematic of plasmids for GR-GFP, GR-GFP 211Ala and GR-GFP 211Asp (A). HeLa cells were transfected with plasmids containing either GR-GFP, GR-GFP 211Ala (B) or GR-GFP 211Asp.(C) Transfected cells were incubated with 100 nM Dex, 3 nM GSK47867A or 3 nM GSK47869A [69A]. Cells were fixed with PFA and analysed for subcellular localisation of the GR-GFP (white) at the times indicated. Images are representative of three independent experiments. Time (mean +/- SEM) taken for the GR to become exclusively nuclear was measured across both the fixed and live cell imaging experiments (D). Statistical significance was evaluated by one way ANOVA followed by Tukey post-test. Asterisks indicate: *$p < 0.001$ significantly different from GR-GFP.

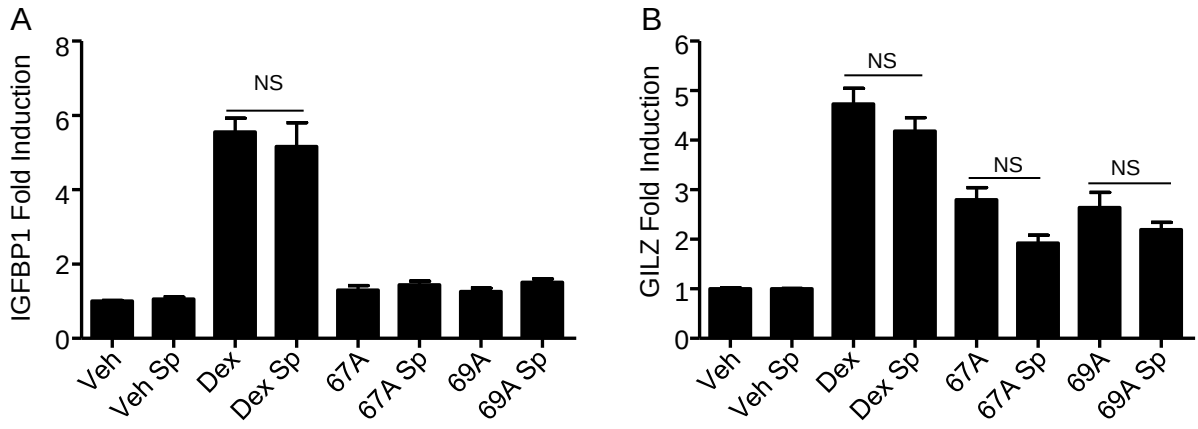

Fig. S11: Endogenous gene regulation in the presence of an MR inhibitor

HeLa cells were pretreated for thirty minutes with 1 uM spironolactone and subsequently treated with DMSO vehicle, 100 nM Dex, 3 nM GSK47867A [67A] or 3 nM GSK47869A [69A] for one hour then lysed and RNA extracted using an RNeasy kit. RNA was reverse transcribed and subjected to qPCR of IGFBP1 (A) and GILZ (B) using Sybr Green detection in an ABI q-PCR machine and data analysed by δδ CT method. graphs (mean ± SEM) combine data from three separate experiments and display fold change over vehicle treated control. Statistical significance was evaluated by one way ANOVA followed by Tukey post-test. NS = not significantly different from treatment without spironolactone.

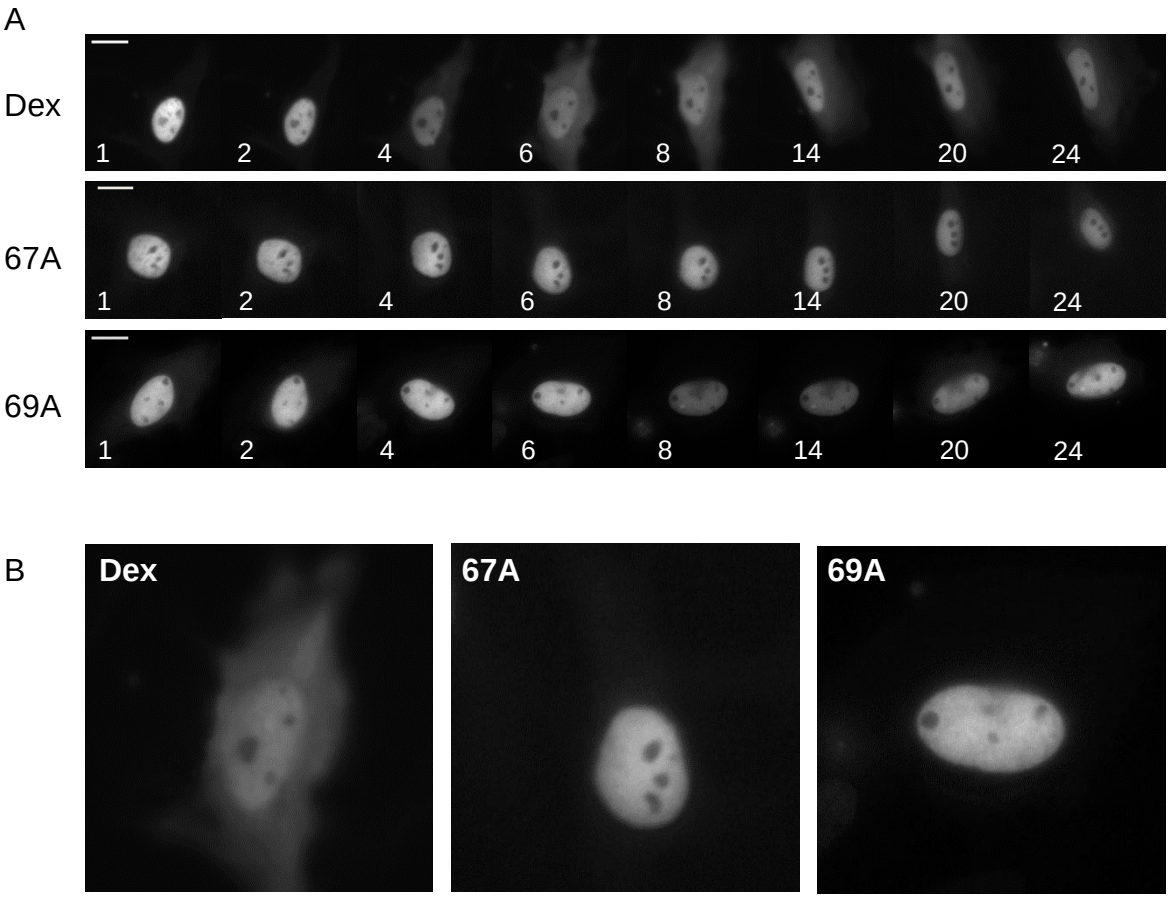

Fig.S12: Nuclear export of the GR
HeLa cells were transfected with GR-GFP and incubated with 100 nM Dex, 3 nM GSK47867A [67A] or 3 nM GSK47869A [69A] for two hours then subsequently washed and imaged for the following twenty four hours to assess subcellular GR localisation (white). Magnification of the six hour time point demonstrates the difference in subcellular GR localisation (B). Scale bar, 25µm. Images are representative of three independent experiments.

Movies 1 and 2. Kinetics of GR translocation at equipotent ligand concentration depicted in Fig. 4C. Following transfection with HaloTag-GR HeLa H2B cells were incubated with (movie 1) 100 nM Dex, (movie 2) 3 nM GSK47867A (67A). Cells were imaged in real time at 37^{o}C to determine the subcellular localisation of the GR (green). The nucleus is shown in blue. Images acquired every minute; frame rate is 20 frames per second. Scale bar, 25 μm.

Movies 3 and 4. Kinetics of preliganded GR depicted in Fig. 5E. Following transfection with HaloTag-GR HeLa H2B cells were placed on ice for 10 minutes and subsequently incubated with (movie 3) 100 nM Dex, (movie 4) 3 nM GSK47867A (67A) for 1 hour on ice. Following treatment cells were imaged in real time at 37^{o}C to determine the subcellular localisation of the GR (green). The nucleus is shown in blue. Images acquired every 3 minutes; frame rate is 20 frames per second. Scale bar, 25μm.

Movies 5 and 6. Export of GR following ligand withdrawal depicted in supplementary material Fig. 12A. HeLa cells were transfected with GR-GFP and incubated with (movie 5) 100 nM Dex, (movie 6) 3 nM GSK47867A (67A) for 2 hours then subsequently washed and imaged for the following 24 hours to assess subcellular GR localisation (white). Images were acquired every 5 minutes; frame rate is 20 frames per second. Scale bar, 25 μm.

Movies 7 and 8. Kinetics of GR translocation following microtubule disruption depicted in Fig. 6F. Following transfection with a halo tagged GR (white) HeLa cells were incubated with 2 μM Colcemid for 1 hour then subsequently co-treated with (movie 7) 100 nM Dex, (movie 8) 3 nM GSK47867A (67A). Cells were imaged in real time and analysed for subcellular localisation of the GR (white). Images were acquired every 2 minutes; frame rate is 20 frames per second. Scale bar, 25μm.